

EFFECTIVENESS OF PHYSICAL DISTANCING IN A MOSQUE DURING CONGREGATIONAL PRAYER USING CFD SIMULATION APPROACH

Siti Najiah Rosminahar*, Mohamad Nur Hidayat Mat, Muhammad Hafizudin Adnan and Wong Keng Yinn

Faculty of Mechanical Engineering, Universiti Teknologi Malaysia, 81310 UTM Johor Bahru, Johor, Malaysia

*Corresponding email: sitinajiah@graduate.utm.my

Article history

Received

10th June 2024

Revised

19th September 2024

Accepted

29th October 2024

Published

29th December 2024

ABSTRACT

This study aims to investigate the effectiveness of physical distancing in a mosque during congregational prayer using the Computational Fluid Dynamic (CFD) simulation approach. A three-dimensional (3D) model of a mosque, prayer, and assailant was designed using Computer Aided Design (CAD) software. Then, a simulation is run using CFD software to simulate the pathogen transmission during the congregation prayer. The simulation is run with the fix of air movement, temperature, and humidity at variable distances, as distancing is the main focus of the study. This is to avoid other factors affecting the results of this study, as what matters the most is the distance among the prayers. The mesh sensitivity study has been done to get a good simulation result that is close to the real world using the numerical computational method. A correct turbulent model is then chosen, and the simulation data obtained were pre validated by the previous literature study. The simulations showed that the pathogen tends to move to the front right side of the mosque. Particles deposition showed that prayer at the front of the assailant received the most percentage of the particles deposition which is the highest 1.3% particles at 3m physical distancing and prayers at the side received least percentage of particles deposition for all physical distancing. The particles also mostly deposited at the ceiling and the mosque's ground. Finally, the result showed that the further distance among the prayers will minimise the virus reproduction number, R_0 value during the congregational prayer. The highest value of R_0 for without physical distancing is 3 at the interval of 40s to 50s, while the value of R_0 for 3m and 4m physical distancing is 0 at the interval of 80s to 100s. This is because the virus cannot be transmitted to many people as the distance between humans increases. The percentage of probability infected prayers is the highest for without physical distancing, which is 26.63% out of total prayers, while at the lowest for 4m physical distancing, which is 14.29% out of all prayers. In conclusion, the pathogen transmission among prayers can be reduced by applying physical distancing as the pathogens are droplet nuclei that are sufficiently small to remain suspended in the air for an extended period and can travel more than 2m distance.

Keywords: Physical distance, Indoor, CFD, simulation, prayer

© 2024 Penerbit UTM Press. All rights reserved

1.0 INTRODUCTION

By late December 2019, a virus outbreak occurred in Wuhan, China, and it was identified as a novel coronavirus. The virus has been temporarily named severe acute respiratory

syndrome coronavirus 2 and later officially named coronavirus disease 2019 (COVID-19) by the World Health Organization (WHO) [1].

Now, COVID-19 has become a pandemic affecting the whole world. One of the preventives measured to prevent the virus from spreading more is a physical distancing prescribed by the WHO, stating that everyone should keep a 1.5 m or 2 m distance between each other to minimise the spread of the virus. However, recent studies show that the virus might be able to transmit over a two (2) m distance [2]. This is due to smaller respiratory droplets ($<5 \mu\text{m}$), which can remain airborne for a longer period and can travel further compared to bigger droplets ($> 100 \mu\text{m}$), which likely can only travel within two (2) m and then fall due to gravity [3].

Therefore, this study will focus on the effect of physical distancing in a confined space area on minimising virus transmission. Since the congregational prayer inside a mosque takes place in a confined space and involves a large number of people, therefore a study inside a mosque is chosen as a model for this study to determine the best physical distancing in minimising the virus transmission from human to human while congregation prayer is done.

2.0 METHODOLOGY

2.1 Simulation Model

Masjid Riyadhus Solihin, located in Seri Kembangan, Selangor was selected to become the model as a confined space area for the simulation process. The selection is made due to the mosque's size, which is not too big for the simulation process, as the time required to process the simulation will not be too long. The 3D model was created using SolidWorks, and the internal model was simplified to reduce the numerical computational load. In addition to this, the mosque also was chosen due to its availability of all mechanical devices such as air conditioners units, wall and ceiling fans to represent general mosques in Malaysia. Next, the 3D model was created by using SolidWorks and the internal of the model has been simplified to reduce the numerical computational load.

The measurements of the mosque are estimated taken by Apple's measurement application as shown in Table 1. The application uses LiDAR Scanner technology which can gauge the size of objects and save the photos of the measurements. So, some errors need to be considered when taking the measurements of the mosque.

Table 1: Simplified the Model's Measurement for reference as designed by SolidWorks

Parameter	Value
Floor plan (L x W x H) (m)	23 x 14 x 2.65
Pulpit (L x W x H) (m)	3 x 3 x 2.65
Pulpit's window (L x H / radius) (m)	1 x 1.2 / 0.5
Pillar (L x W x H) (m)	0.2 x 0.2 x 2.65

The 3D model was then constructed by using SolidWorks software in Figure 1, and all the doors and windows were neglected as they were closed during the congregation prayer. The air conditioners were also attached to the wall of the building while the ceiling fans and ceiling were added during the CFD process.

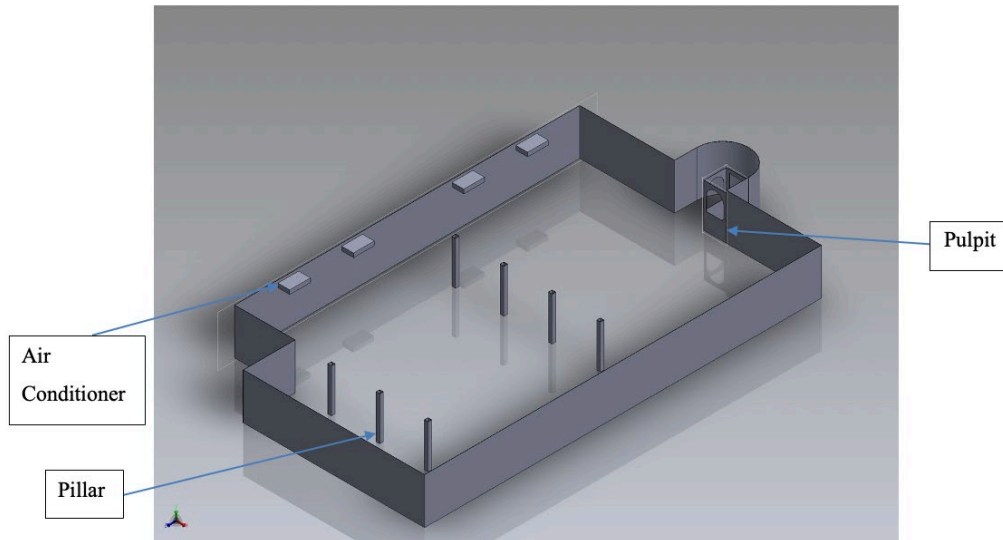


Figure 1: SolidWorks 3D Model of the Mosque

Eight (8) ceiling fans and four (4) air conditioners are used inside the mosque. The model used for the ceiling fans is from KDK K15VC (150cm) [6], and the model for the air conditioners is Daikin FHC60AV1M [7]. All fans and air conditioners are switched on during the congregation prayer. All the operating conditions for the fans and air conditioners are in Table 2.

Table 2: Fans and Air Conditioners Operating Conditions

Parameter	Value
Number of ceiling fan	8
Number of air conditioner	4
Volume flow rate of ceiling fan	230 m ³ /min
Volume flow rate of wall fan	17.56 m ³ /min

The prayer and assailant are constructed as a 3D model of a simple mannequin and its dimension is presented in Table 3. Only essential parts are considered during the construction of the 3D model: body, head, and mouth.

Table 3: Prayer's/Assailant's Measurement

Parameter	Value
Body (H x L x W) (mm)	1600 x 450 x 250
Head (H x L x W) (mm)	250 x 200 x 200
Mouth (H x L) (mm)	10 x 40

The study considered that only one assailant coughed once at the centre of the mosque. The main variable to be studied is the distancing between the prayers. All the operating conditions for the cough are in Table 4.

Table 4: Prayer/Assailant Operating Conditions

Parameter	Value	Source
Size of coughing droplets	1-1000 μ m	Ho, C.K., 2021 [3]
Type of particle diameter	Gaussian	Ho, C.K., 2021 [3]
Quantity of droplets	3000	Ho, C.K., 2021 [3]
Velocity of droplets	11.2 m/s	Kwon et al., 2012 [5]
Initial velocity of droplets	25 m/s	Kwon et al., 2012 [5]
Reynolds number	10000	Ho, C.K., 2021 [3]
Mouth opening	4cm ²	Ho, C.K., 2021 [3]
Density	1000 kg/m ³	Refer to distilled water

The air flow circulation inside the mosque is predicted by using CFD simulation approach. The CFD simulation is conducted using a CFD solver, scFLOW student edition. The airflow circulation process followed the continuum fluid model, and this applies to the governing equations which are conservation of mass, momentum, and energy [4]. The equations require operating condition as prepared in Table 5. Transient state analysis is selected to monitor the spread of pathogen transmission during the conducting of the CFD simulation. The pathogen originated from the location of the mouth of the assailant and only coughed once. The distancing between the prayers will be varied to study the effectiveness of physical distancing in a mosque during congregational prayer. Each of these distances are going to be tested under the same conditions. This is to avoid other factors affecting the results of this study as what matters the most is the distance among the prayers. The Figure 2 and Figure 3 represent the prayer arrangement set to 1-meter and 3-meter physical distancing.

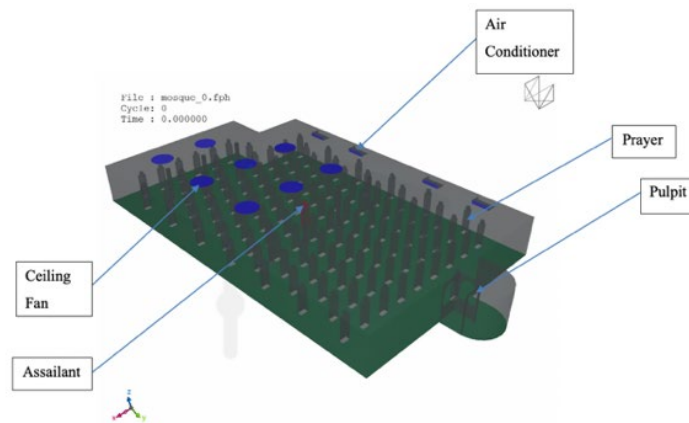


Figure 2: Prayer Arrangement 1 Meter

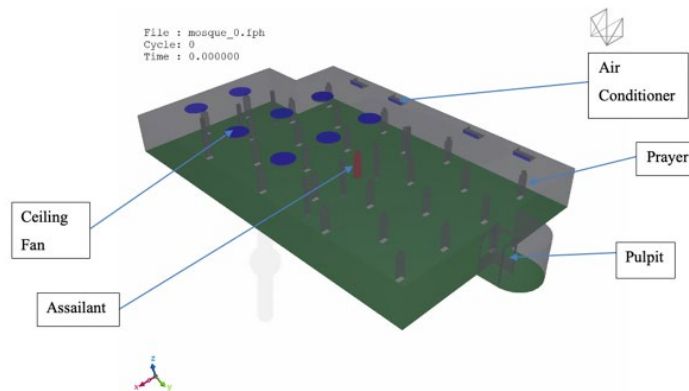


Figure 3: Prayer Arrangement 3 Meter

Table 5: CFD Simulation Operating Condition

Parameter	Value	Source/Note
Analysis type	Transient	Ho, C.K., 2021 [3]
Type of flow	Turbulent	Ho, C.K., 2021 [3]
Turbulent model	LES	Turbulent Model Selection
Number of cycles	1000	Try and error analysis
Time steps	0.1s	Try and error analysis
Exhaled air temperature	37°C	Ho, C.K., 2021 [3]
Exhaled air humidity	100%	Ho, C.K., 2021 [3]
Ambient temperature	20°C	Ho, C.K., 2021 [3]
Ambient humidity	50%	Ho, C.K., 2021 [3]

2.2 Mesh Sensitivity Study

The meshing process is one integral part of whenever engineering simulations are used. Usually, meshing involves complex geometries divided into simple elements used as discrete local approximations of larger domains. Meshing is vital as it determines the accuracy, speed, and convergence of the simulation.

A fine meshing statistic is used as a fine mesh provides much better accuracy than a medium and coarse mesh. A few settings have been done based on the design to suit the study. The maximum size of the mesh is set to 300 mm around the prayer and assailant body, and the minimum size near the mouth is 40 mm, with a growth rate of 1.2. The mesh gets smaller as it approaches the area of the mouth and nose, which are the most vulnerable parts of the human body to pathogens. as shown in Figure 4.

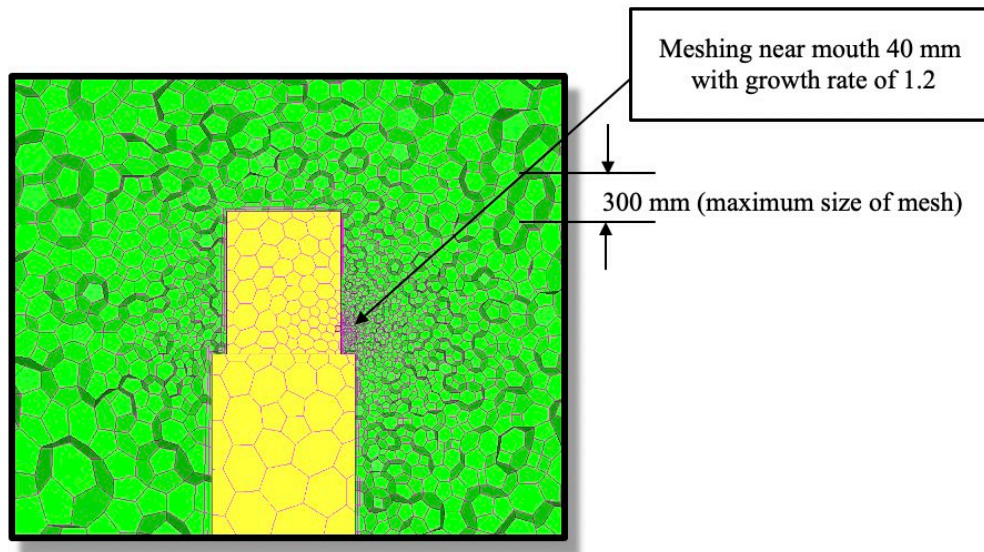


Figure 4: Zoom View of Polyhedral Mesh

The mesh is classified into three different categories of mesh, which is fine mesh, medium mesh and coarse mesh. The classification is determined by calculating the representative cell length, h , which is the average element size for all meshes in the domain. As it is a 3D model, the h is calculated by the equation (1) :

$$h = \frac{1}{N} \sum_{Cells} V_p^{1/3} \quad (1)$$

It is more effective to know the value of h compared to the number of cells, N , as the value of h reaches zero as the mesh becomes infinitely small, which is the ideal mesh, and N will become infinity for this mesh. The velocity, v , for each mesh, is then obtained after the simulation by using SST turbulent model, and a graph of h against v is plotted to obtain the velocity at $h = 0$, using the Richardson extrapolated method. This method required many iteration processes to reach the final value. The Richardson extrapolated error is required as the simulation of the smallest mesh size takes a very long time and requires a very high computational load to produce.

The value then is compared with the three different mesh to get the relative error by using the equation (2) :

$$e_{21}^{extr} = \left| \frac{\varphi_1 - \varphi_0}{\varphi_0} \right| \quad (2)$$

As the error obtained is less than 15% as shown in Table 6, the final value of velocity by using this method is accepted.

Table 6: Velocity Value for Each Mesh

Mesh Size	Representative Length (mm)	Velocity (m/s) Present Simulation (SST)	Extrapolated Relative Error
Infinitely Small	0	12.57	Reference
Fine	10.06	13.08	4.06%
Medium	14.64	13.55	7.49%
Coarse	20.83	14.38	13.36%

2.3 Selection of Turbulent Model

As most natural flows are turbulent, a turbulent flow model is required to do the CFD simulation to estimate the model's fluid flow. Three common types of turbulence models are selected: K-Epsilon, Spalart Almaras, and Large Eddy Simulation (LES) model as shown in Figure 5. The simulation uses all three models, and the velocity parameter is obtained. Based on the simulations at 1.7 m height, the velocity values for K-Epsilon, Spalart Almaras, and LES were 14.985 m/s, 15.586 m/s and 12.14 m/s respectively. The values are then compared to the experiment data from the research of Kwon et al. [5], stating that the experimental value of the velocity at 1.7 m height was about 11.64 m/s. The 1.7 m height was chosen as it is the average height for the location of the mouth and nose; this location is the most vulnerable part of the human body to the pathogen. From Figure 5, the best projection turbulent mode for the velocity is the LES model, so the LES model is chosen for this study.

as presented in Table 7.

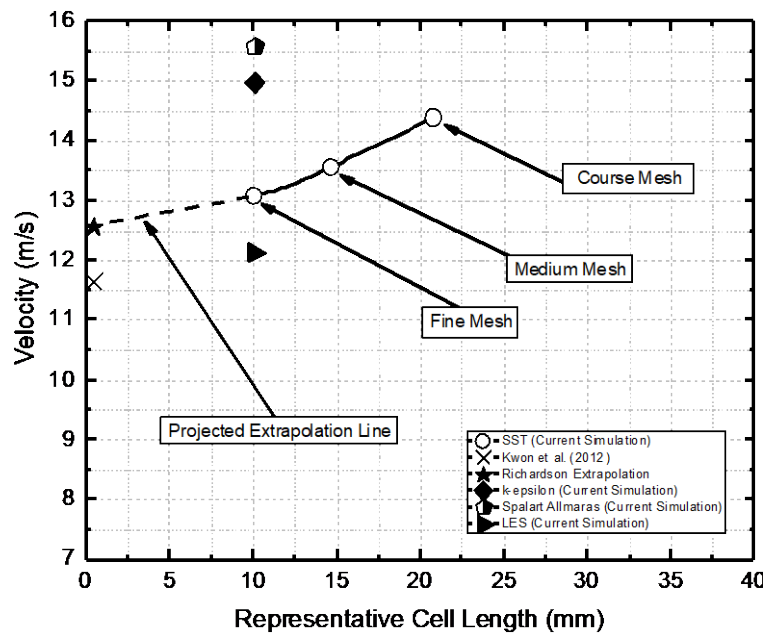


Figure 5: Mesh Refinement Plot of Three Mesh Categories against Velocity

Table 7: Turbulent Model Selection for Velocity Measured at 1.7 m Height

Velocity (m/s) Kwon et al. (2012)	Velocity (m/s) (k-epsilon) P.S *	Velocity (m/s) (Spalart Allmaras) P.S *	Velocity (m/s) (LES) P.S *
11.64	14.985	15.586	12.14

P.S* = Present Simulation

2.4 Mathematical Model

The governing equations used in the present research is the conservation of mass, momentum, and energy. The equations are as follows:

Conservation of Mass as in equation (3)

$$\frac{\partial \rho}{\partial t} + \nabla \cdot (\rho v) = 0 \tag{3}$$

Conservation of Momentum as in equation (4)

$$\rho \frac{\partial U_j}{\partial t} + \rho U_t \frac{\partial U_j}{\partial x_t} = -\frac{\partial P}{\partial x_j} - \frac{\partial \tau_{tj}}{\partial x_i} + \rho g_j \tag{4}$$

Conservation of Energy as in equation (5)

$$dU = \delta Q - \delta W + u' dM \tag{5}$$

2.5 Preliminary Validation Analysis

The preliminary validation process in this study is by using benchmark test by comparing the simulation data with the experimental data obtained by the research of Kwon et. al. So the simulations for other heights are then ran and the values of velocity at other different heights are obtained. . All the values are then compared with the experimental data. Table 8 shows the velocity data at different heights.

Table 8: Experimental Preliminary Validation

Height	u-Velocity outlet (Kwon 2012)	u-Velocity outlet (LES Present)	Relative Error (%)
1.60	7.72	8.02	3.89%
1.65	9.68	10.08	4.13%
1.70	11.64	12.14	4.30%
1.75	13.60	14.25	4.78%
1.80	15.56	16.33	4.95%

3.0 RESULT AND DISCUSSION

3.1 Aerosol Particles Spreading Characteristics

The particle transportability pattern is used to investigate the aerosol particles spreading characteristic, representing the pathogen transmission inside the mosque as demonstrated in Figure 6. The pattern chosen is at 100s time as it is the most significant time to be studied. The characteristic of the particles spreading under transient state can be determined by knowing the pattern.

The top view of the particle transmission for the magnitude of the velocity of the particles at 100s time without distancing, 1m, 2m, 3m, and 4m distancing are presented in Figure 6. The significant finding reveals that the pathogen tends to move to the front left side of the mosque without physical distancing. However, with physical distancing of 1m until 3m, the pathogen tends to move to the front right side of the mosque. However, with 4m distancing, the pathogen can move to the middle right of the mosque. The pathogen transmissions most of the time are to the right side of the mosque, which might be due to the position of the air conditioners on the left of the mosque, and the flow from them pushes the pathogen to the right of the mosque. Meanwhile, the prayers might block the flow with no distancing, causing the pathogen transmission to the front left of the mosque. Adwibowo A (year) mentions that the flow of the particles is affected by the seating configuration [12] and supports the finding in the simulation. The pathogen also did not move to the rear of

the mosque for all simulations, and this might be caused by the positioning of the fans that are only placed at the rear of the mosque, preventing the pathogen from moving to the rear. As the ceiling fan's volume flow rate is higher than air conditioners [6,7], particles are pushed to the mosque's front side. This simulation of the particle transmission also proves that the pathogen can travel further than 2m, as stated by Setti, L. et al. and up to 4m distance [2].

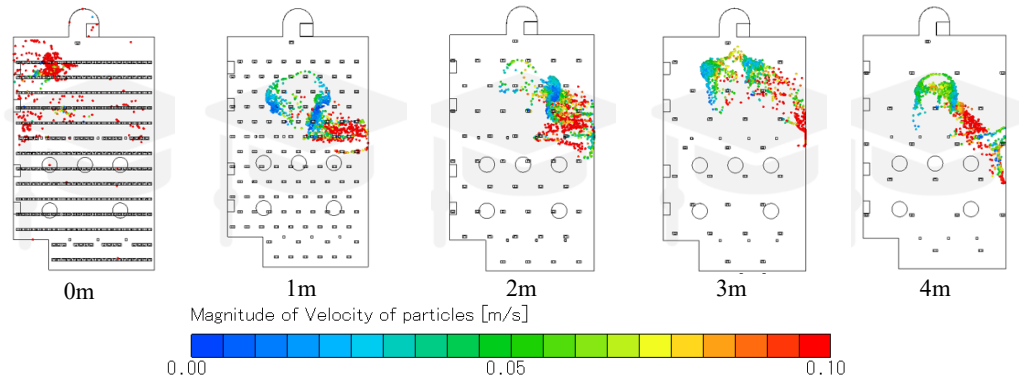


Figure 6: Magnitude of Velocity of Particles for different Physical Distancing

The magnitude of the velocity of air circulation at 100s times is also considered to understand the pathogen transmission behaviour further. The particle velocity vector of air conditioners and fans for all five (5) physical distancing are demonstrated in Figure 7. The air velocity vector for all simulations is the same except without physical distancing. Figure 7 shows that the highest velocity are at the middle of the mosque for the prayers without physical distancing. In contrast, the prayers with physical distancing show that the highest velocity vector is from the middle to the front of the mosque. The air circulation from the air conditioners and the fans causes this velocity vector. M.N.H. Mat (2021) mentions that fan activation influences pathogen transmission and deactivation due to the propagational energy of the fan flow [8]. This finding can verify the pathogen transmission discussed before.

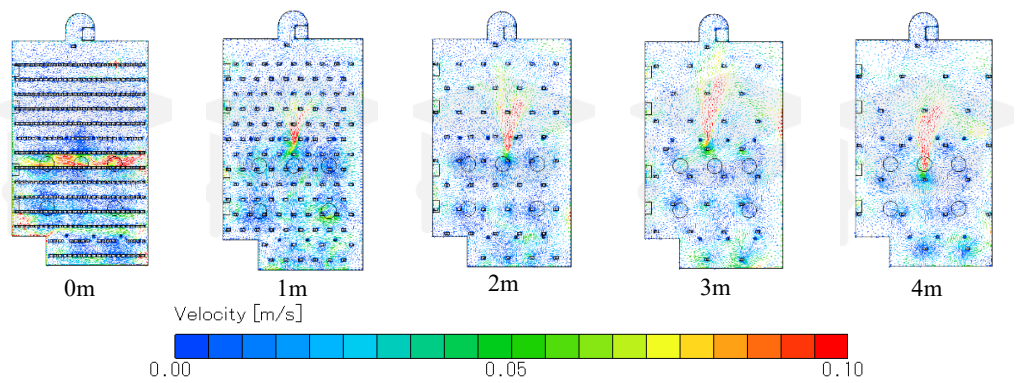


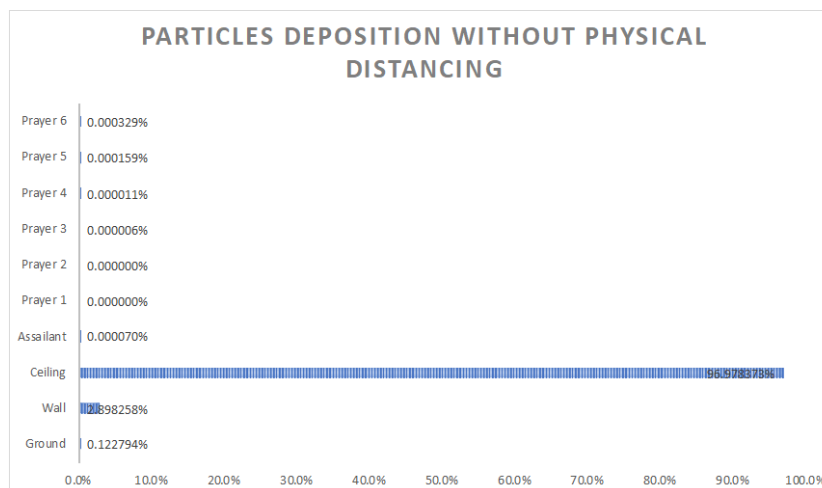
Figure 7: Magnitude of Velocity of Air Circulation for different Physical Distancing

3.2 Particles Deposition

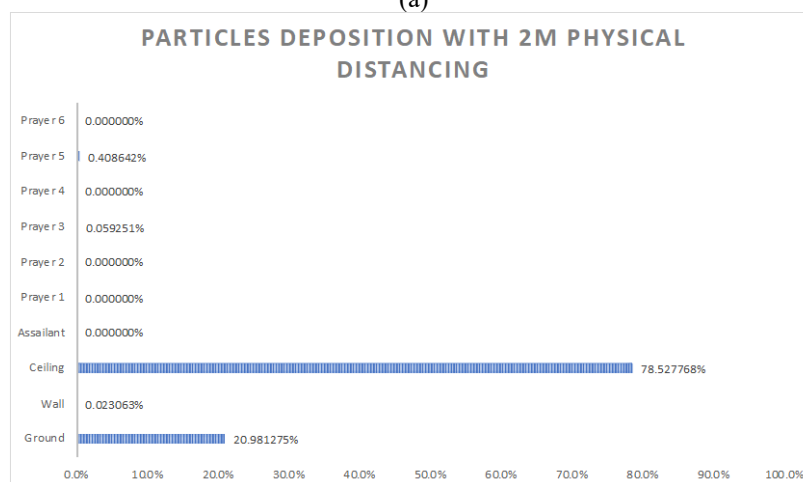
The particle deposition shows how much particles are touching the prayers and the surroundings of the inside of the mosque. The entities chosen for the particle deposition study are the assailant, six (6) prayers located at the side and front of the assailant, ground, wall, and ceiling. The particle deposition data is extracted, and the percentage of the particles is calculated for each entity chosen out of the total of all entities. From the data

extracted, bar graphs show the percentage of the particle's deposition. Figure 8 shows the percentage of particles touching the assailant, six (6) prayers located at the side and front of the assailant, ground, wall, and ceiling for different physical distancing. Prayer 1 and Prayer 2 mostly had the lowest percentage of particles touching them as they were at the assailant's side. The other prayers received a higher percentage of particle deposition because they were at the front of the assailant. As the pathogens are mainly transmitted to the front of the mosque, these prayers received a higher percentage of pathogen touching them than the prayers at the side. Prayer 3 gains the highest percentage of particle deposition with 3m physical distancing at around 1.3% of total particles. The result can be supported by a paper by M.N.H. Mat that states prayer at the front of the assailant receives the highest number of particle depositions [8].

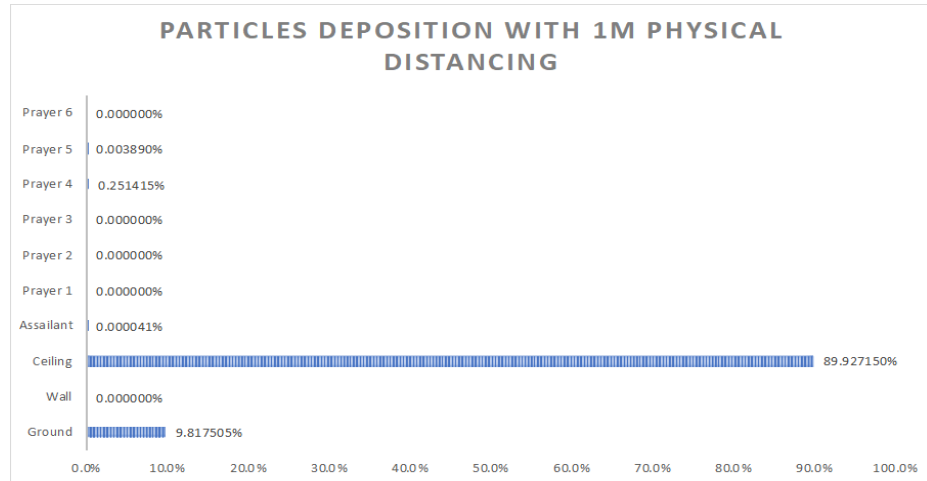
However, most of the particles are deposited at the ceiling and the ground for all five (5) different physical distancing, with mostly the highest percentage of particle depositions at the ceiling except for the ground at 3m physical distancing. The highest percentage of particle deposition for the ceiling is without physical distancing with 96.9% particle deposition, while the lowest is 30.9% at 3m physical distancing. It might be due to the highest concentration of pathogens in the air due to the flow of air conditioners and the fans. This result can be related to a study by Yang., et al. and Ho, C.K. and, that smaller respiratory droplets (<5 µm) can remain airborne for a longer period [11,3] and can travel further compared to bigger droplets (> 100 µm) which likely can only travel within 2m and then fall down due to the gravity [3]. This means that the smaller droplets tend to move upward to the ceiling while the bigger droplets drop down to the ground.



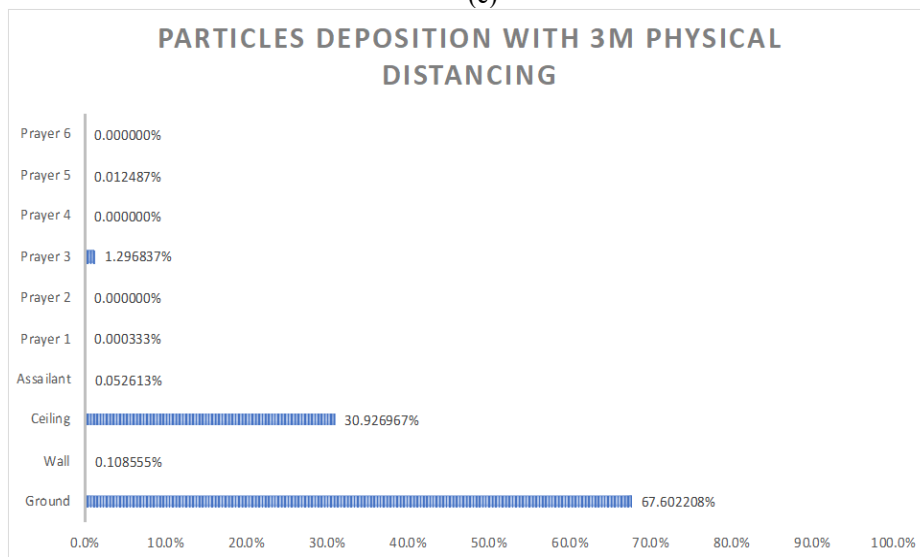
(a)



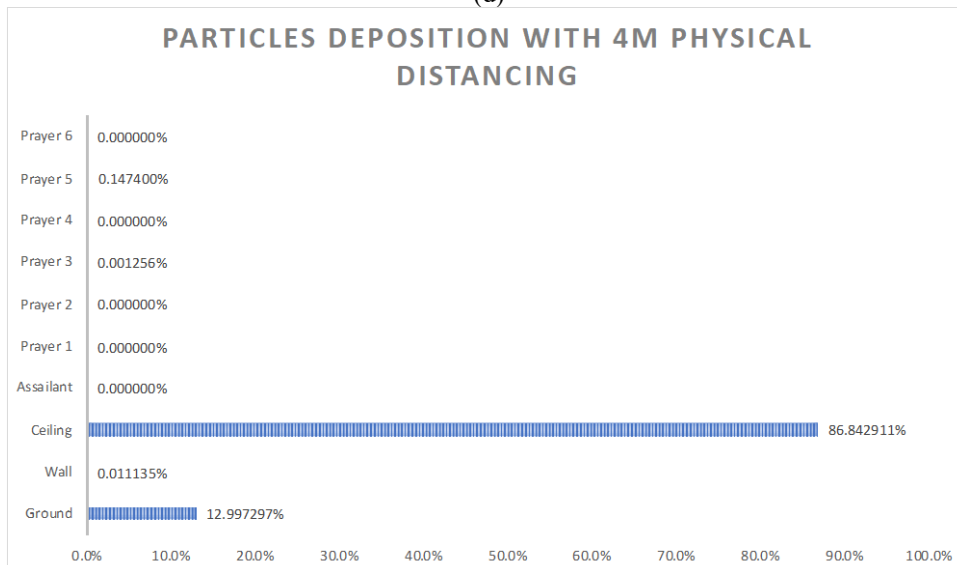
(b)



(c)



(d)



(e)

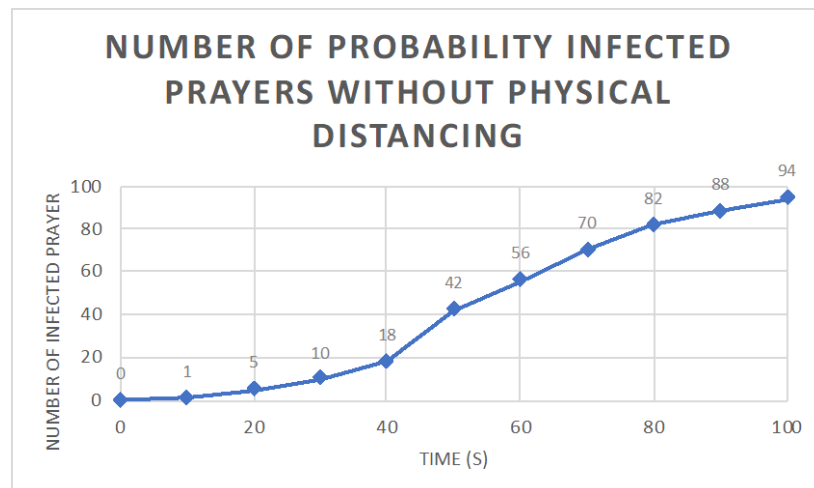
Figure 8 (a-e): Particles Deposition for different Physical Distancing

3.3 Virus Reproductive Number

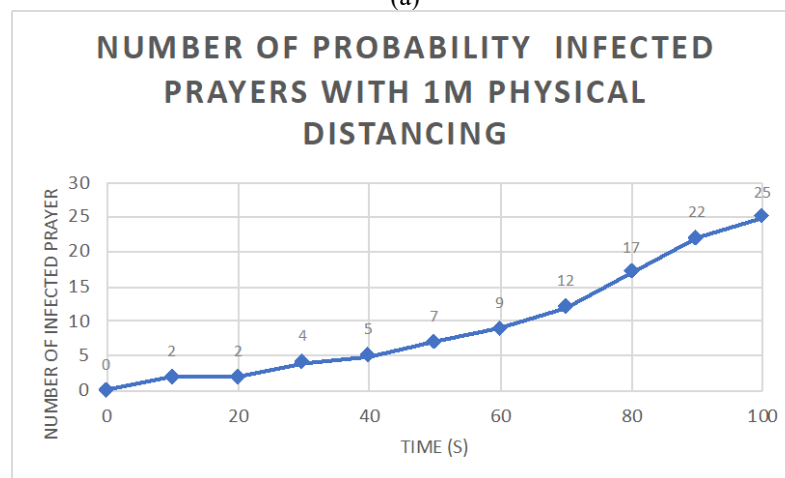
The number of probability infected prayers with respect to time for 5 different physical distancing are represented in Figure 9. The number of probability infected prayers is gradually increasing over time for all distancing with higher value for without physical distancing compared to 4m physical distancing.

For the simulation without the physical distancing, the number of probability infected prayers constantly increasing from 0s until 100s. The number increases drastically between 40s to 80s then started to slow down a bit. The highest value of R_0 for without physical distancing is 3 which is at interval of 40s to 50s. The same pattern can be seen for 1m physical distancing, which shows that the probability of infected prayers keeps on increasing over time. For 2m physical distancing, the probability of infected prayers hardly increases from 0s to 50s, but then the number increases remarkably until 100s.

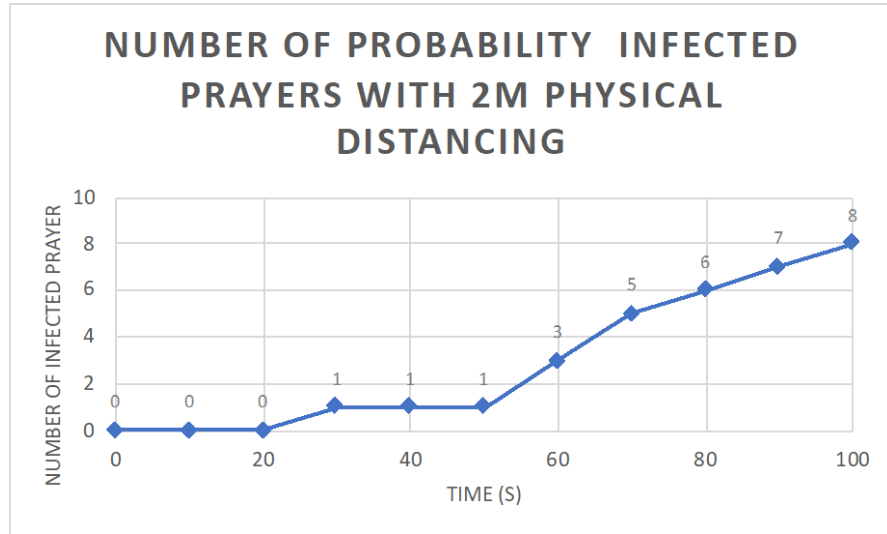
However, the pattern for the 3m and 4m physical distancing shows different patterns from the pattern of simulation for the without physical distancing, 1m, and 2m physical distancing. Figure 9 shows that the number increases 0s to 40s and then remain stagnant until 60s, then increases until 80s, and remains the same again until 100s. The same pattern can be seen for the simulation for 4m physical distancing which is the value remain the same from 0s until 40s then started to increase until 80s then the number of infection prayer continue to be the same again. The value of R_0 for 3m and 4m distancing is 0 at the interval of 80s to 100s. This finding can be supported by Kucharski, A.J., et al and Jarvis, C.I., et al that stating the physical distancing can reduce the reproductive number of infected persons [9,10].



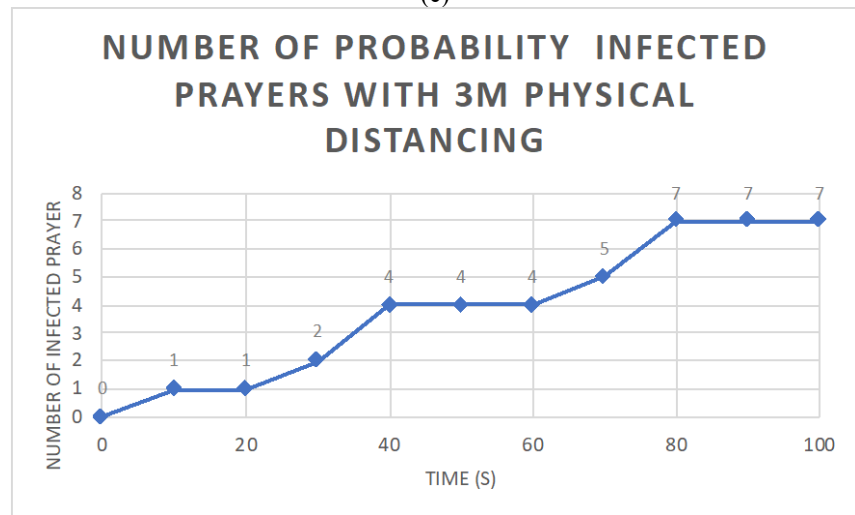
(a)



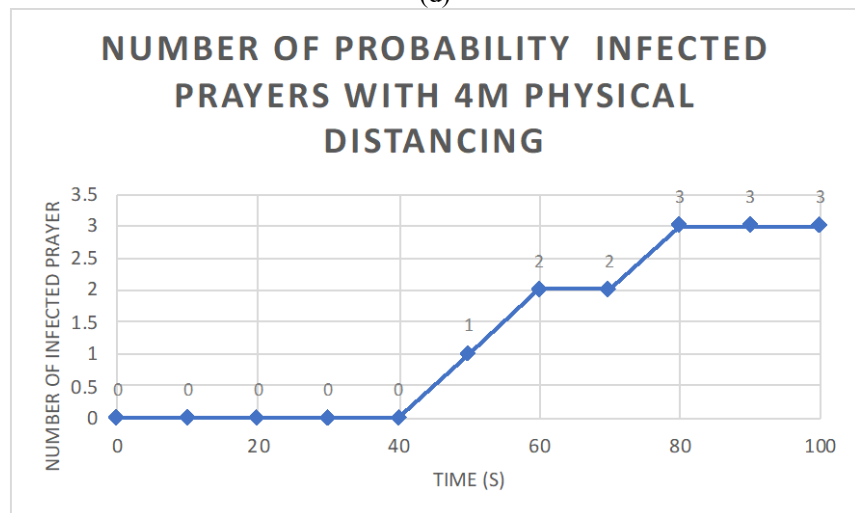
(b)



(c)



(d)



(e)

Figure 9: Number of probability Infected Prayers for different Physical Distancing

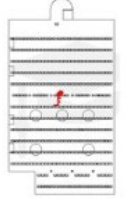




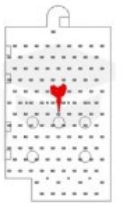
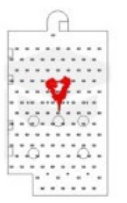
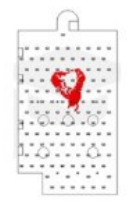
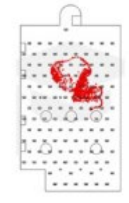
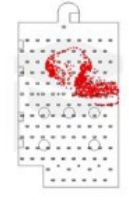

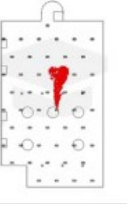
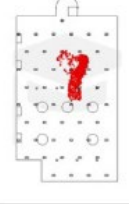
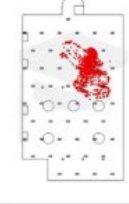
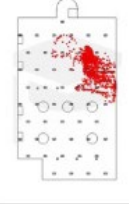
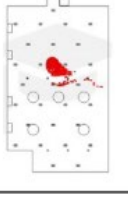
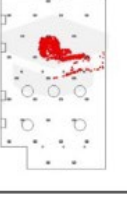
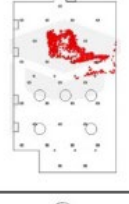
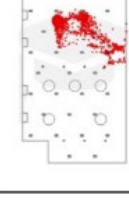
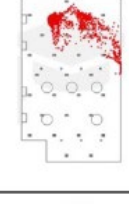
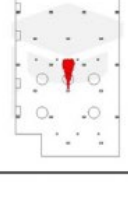

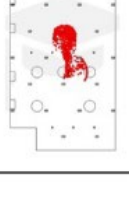
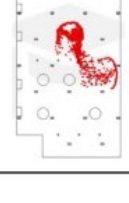
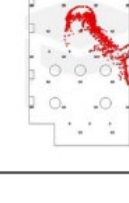
Table 9: Percentage of Probability Infected Prayers at 100s time

Physical Distancing	Percentage of Probability Infected Prayer	Total Prayers
Without Physical Distancing	26.63%	353
1m	21.01%	119
2m	16.33%	49
3m	25.00%	28
4m	14.29%	21

Finally, at 100s time, the percentage of probability infected prayers for each physical distancing is calculated to compare how many prayers are probably infected out of the total of the prayers. The percentage of the probability infected prayers gradually decrease from without physical distancing to 2m physical distancing. But the percentage increases for 3m physical distancing. However, the percentage is decreasing again for the 4m physical distancing. The highest percentage of probability infected prayers is at without physical distancing meanwhile the lowest percentage is at 4m physical distancing. Jarvis, C.I., et al also found 74% reduction in the average daily number of contacts observed per participant when physical distancing was adopted [10] proving that when the physical distancing is applied, the percentage of infected people decreasing.

The virus spreading transmission from the top view for every physical distancing at intervals of 20s are demonstrated at Table 10. The red colour represent the virus particles transmission over the time. The virus transmission starts at the middle of the mosque for all physical distancing. The virus then gradually start moving to the front of the mosque and manage to cover around 25% of the area of the mosque at 60s time. The virus transmission follows the pattern of air velocity circulation at chapter 3.1. The transmission mostly affected by the air flow of air conditioners and fans of the mosque. A quite similar pattern can also be found in paper wrote by Mohamadi, F. and A. Fazeli [13].

Table 10: Direction of Virus Spreading from the Top View

Physical Distancing	Duration				
	20s	40s	60s	80s	100s
Without Physical Distancing					
1m					
2m					
3m					
4m					

4.0 CONCLUSION

In conclusion, the pathogen transmission among prayers can be reduced by applying physical distancing as the pathogens are droplet nuclei that are sufficiently small to remain suspended in the air for an extended period and can travel more than 2m distance. The pathogen can still travel through air for over 2m distances and in this study up to 4m physical distancing. In recommendation, the physical distancing among prayers need to be applied in the time of pandemic to reduce the virus infecting more people.

The study uses a simulation of the virus transmission in a confined space, inside a mosque. Therefore, this study can also be used to investigate the virus transmission in other confined places with similar conditions, such as in cinema, which is a closed space with the person not moving for a long time. The cinema also commonly used air conditioners

like the mosque in this study, so the spreading characteristic might be quite similar to the result obtained from the simulation. However, if the confined space consists of constantly moving people, this analysis might not be accurate to be used. Therefore, understanding the nature of the space could help to compare this finding with other spaces.

However, every research has its own flaws and limitations. For every 3000 droplets of coughing [3], it is not definitely that all particles contained the virus, so not all prayers that have contact with the particles is confirmed to be infected by the virus. The contact also considered at all over the body of the prayers not specified in the dangerous area like in the face area, so the prayers that have contact are only have some possibilities to be infected by the virus. Furthermore, the simulations only consider constant environmental conditions such as constant wind velocity, temperature, and humidity whereas the real world all the conditions are not constant all the time. The simulations also only consider the assailant only cough once while in real life the assailant might coughing more than once.

Hence, there are still more room for improvements to be done to get more accurate result. Some of the recommendations that could be done for the next study are:

- i) Develop more real 3D modelling of the confined space to get more accurate result.
- ii) Do real-world experiments for final validation of this study.
- iii) Perform simulations with higher number of mesh to get more accurate result.
- iv) Find the exact number of viruses in the coughing droplets.
- v) Specified the area that are vulnerable for the virus to infect human.

ACKNOWLEDGEMENTS

This research was sponsored by Ministry of Higher Education (MOHE) through Fundamental Research Grant Scheme (FRGS/1/2021/TK0/UTM/02/98).

REFERENCES

1. He, F., Y. Deng, and W. Li, *Coronavirus disease 2019: What we know?* Journal of medical virology, 2020. **92**(7): p. 719-725.
2. Setti, L., et al., *Airborne transmission route of COVID-19: why 2 meters/6 feet of inter-personal distance could not be enough.* 2020, Multidisciplinary Digital Publishing Institute.
3. Ho, C.K., *Modeling airborne pathogen transport and transmission risks of SARS-CoV-2.* Applied mathematical modelling, 2021. **95**: p. 297-319.
4. Mat, M.N.H., et al., Optimizing nozzle convergent angle using central composite design on the particle velocity and acoustic power level for single-hose dry ice blasting nozzle. Journal of Thermal Analysis and Calorimetry, 2020: p. 1-15.
5. Kwon, S.-B., et al., Study on the initial velocity distribution of exhaled air from coughing and speaking. Chemosphere, 2012. **87**(11): p. 1260-1264.
6. Ceiling fan by KDK, <https://www.kdk.com.my/product/k15vc/>
7. Air Conditioner by Daikin, https://www.daikin.com.my/daikin_products/fhc-a-series/
8. Mat, M.N.H., M.F.M. Basir, and E.M. Yusup, Fans deactivation for minimisation of airborne pathogen transmission: During Malaysians congregational prayer gathering in mosque. International Communications in Heat and Mass Transfer, 2021. **129**: p. 105694.
9. Kucharski, A.J., et al., Effectiveness of isolation, testing, contact tracing, and physical distancing on reducing transmission of SARS-CoV-2 in different settings: a mathematical modelling study. The Lancet Infectious Diseases, 2020. **20**(10): p. 1151-1160.
10. Jarvis, C.I., et al., Quantifying the impact of physical distance measures on the transmission of COVID-19 in the UK. BMC medicine, 2020. **18**(1): p. 1-10.
11. Wang, Y., G. Xu, and Y.-W. Huang, Modeling the load of SARS-CoV-2 virus in human expelled particles during coughing and speaking. PLoS One, 2020. **15**(10): p. e0241539.
12. Adwibowo, A., Computational fluid dynamic (CFD), air flow-droplet dispersion, and indoor CO2 analysis for healthy public space configuration to comply with COVID 19 protocol. medRxiv, 2020.
13. Mohamadi, F. and A. Fazeli, A Review on Applications of CFD Modeling in COVID-19 Pandemic. Archives of Computational Methods in Engineering, 2022: p. 1-20.